World Journal of Engineering Research
Print ISSN: 2959-9865
Online ISSN: 2959-9873
DOI: https://doi.org/10.61784/wjer3140

HEATING CHARACTERISTICS OF A SOLAR-CO_2 AIR SOURCE HEAT PUMP COUPLED SYSTEM WITH VALLEY-ELECTRICITY HEAT STORAGE

RuiFang Guo*, ZhanJun Sha
Yinchuan Energy College, Yinchuan 750105, Ningxia, China.
**Corresponding Author: RuiFang Guo*

Abstract: Taking the heating system of a rural household in Yinchuan as the research object, a simulation model of a solar-CO_2 air source heat pump heating system was developed based on TRNSYS, and its operation from November to March of the following year was simulated and analyzed. The results show that the system can reliably satisfy the indoor winter heating demand of rural households, with heating temperature fluctuating little and remaining stable at approximately 18.0 ℃. Regarding the electricity consumption of the coupled system, the energy use of the space-heating pump and the heating circulation pump rises in step with the extreme-cold heat load in winter, showing a pronounced negative correlation with outdoor temperature; in contrast, the energy consumption of the solar collector pump is governed solely by solar irradiation and remains stable throughout the entire heating season. Over the whole heating season, the collector harvested 6,276.26 kWh of heat and the air source heat pump delivered 6,359.19 kWh, the two contributions being nearly equal, with the total heat output of the heat pump slightly exceeding that of the solar collector. The carbon emissions of the solar-coupled heat pump heating system are only 1,433.94 kgCO_2, equivalent to 24.5% of those of a coal-fired boiler (the highest-emitting option), demonstrating remarkable energy-saving and emission-reduction effects. This study aims to refine the theoretical framework of solar-CO_2 heat pump coupled heating and to provide data support for the engineering design and operation-and-maintenance optimization of clean heating projects for residential and public buildings in cold regions.
Keywords: Solar energy; CO_2 air source heat pump; TRNSYS; Heating performance

1 INTRODUCTION

Against the backdrop of global shifts in energy structure and energy demand, coupled with the goals of carbon peaking and carbon neutrality, it has become urgent to explore sustainable and clean heating solutions. Conventional heating methods such as coal-fired and oil-fired boilers not only consume massive fossil fuels but also cause severe environmental pollution. Solar energy, as a clean and renewable energy source, boasts enormous development potential. In particular, Ningxia is endowed with abundant solar energy resources. Air-source heat pump technology can efficiently extract low-grade heat from ambient air and upgrade it into high-grade heat for heating purposes, featuring a relatively high coefficient of performance (COP) [1]. As a natural refrigerant, carbon dioxide exhibits distinctive merits including environmental benignity, high safety and superior heat transfer performance. In 2013, the Department of Housing and Urban-Rural Development and the Development and Reform Commission of Ningxia Hui Autonomous Region jointly issued the Implementation Plan for Carbon Peaking in the Urban-Rural Construction Sector of Ningxia Hui Autonomous Region. The plan advocates the localized promotion of complementary multi-energy technologies integrating solar energy and air-source heat pumps to advance clean heating. Accordingly, the heating system combining solar energy and CO_2 air-source heat pumps is expected to offer a novel pathway to address energy and environmental challenges within the heating sector [2].

At present, many researchers at home and abroad have investigated the performance of heating systems that integrate solar energy and air-source heat pumps. Wang Yanan et al. established simulation models of series and parallel solar heat pump hot water systems using TRNSYS, and simulated and analyzed the operational performance of the two systems on typical days and throughout the whole year in Xi'an [3]. The results revealed that on typical days in summer and transition seasons, given the same collector area, the parallel configuration The daily average operational efficiency of the parallel system was higher than that of the series system for most of the year in Xi'an, and only slightly lower on typical winter days. The parallel system achieved a substantially better annual efficiency and lower energy consumption than the series one. Furthermore, Zeng Naihui built a model of an air-source heat pump assisted solar hot water system on TRNSYS and optimized its key parameters [4]. The optimized system exhibited overall performance improvement, reduced annual operating cost, and an annual electricity saving rate up to 9.11%. X. R. Zhang et al. designed and constructed a solar heat collection system using CO_2 as the working fluid and carried out experimental analysis [5]. Experimental results demonstrated that the temperature, pressure and mass flow rate of CO_2 rose with increasing solar radiation, which differed from solar collector systems with conventional working fluids. The annual average efficiency of the solar collector exceeded 60.0% when CO_2 was adopted as the working fluid. Kim et al. proposed a solar heating system with a CO_2 heat pump as the auxiliary heat source to satisfy domestic hot water and space heating demands [6]. In this system, the solar thermal storage tank served as the heat sink for the CO_2 heat pump. When solar energy failed to

© By the Author(s) 2026, under the CC BY-NC-ND license (http://creativecommons.org/licenses/by-nc-nd/4.0).

meet the hot water and heating loads due to weather conditions, the CO_2 heat pump extracted heat from the ambient environment to heat the water in the tank and delivered the heat to the demand side. Nevertheless, Kim et al. mainly focused their research on the performance of the CO_2 heat pump unit [7-8].

This paper takes the solar-coupled transcritical CO_2 air-source heat pump heating system as the research object, establishes a complete system simulation model, analyzes the variation laws of the system heating capacity, heating coefficient of performance and energy consumption during the heating period, and clarifies the energy coupling and transfer characteristics of the system under multiple working conditions.

2 COMPOSITION AND OPERATION MODE OF SOLAR-CO_2 AIR-SOURCE HEAT PUMP SYSTEM

The solar-CO_2 air-source heat pump system is a composite heating system that couples the solar heat collection subsystem with an air-source heat pump using CO_2 as the working fluid. This paper mainly investigates the parallel operation of the solar-CO_2 air-source heat pump system. Its working principle is shown in Figure 1-2:

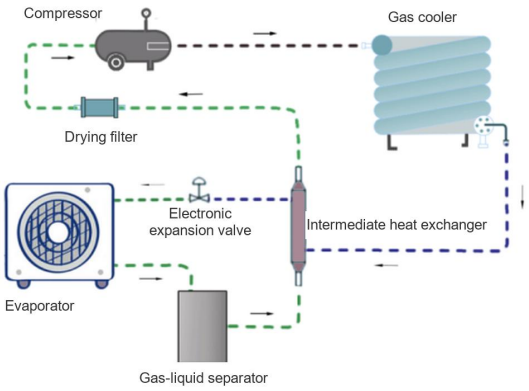


Figure 1 Working Principle of CO_2 Heat Pump

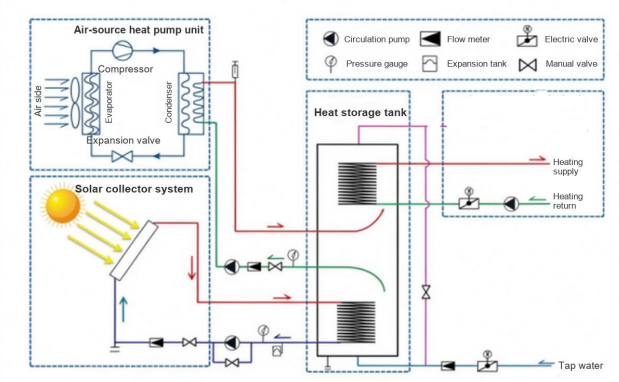


Figure 2 Working Principle of the Combined System

As a refrigerant, CO_2 is environmentally friendly and non-toxic, and it can produce high-temperature hot water under heating conditions. This paper mainly investigates the transcritical CO_2 cycle, in which the evaporation process of CO_2 occurs below the critical point and the heat rejection process takes place above the critical point, so that no phase change occurs during the heat rejection process.

An automatic control system is required for the solar-coupled air-source heat pump system. On the one hand, solar energy is unstable with large fluctuations in solar irradiance. To achieve continuous and stable heat supply, the automatic control system switches between different heating modes to ensure safe and continuous system operation. On the other hand, each component of the system has specific requirements for the working fluid temperature; the control elements in particular are temperature-sensitive. Therefore, protective control is configured to prevent overheating and other faults.

2.1 System Operation Control

System operation control is divided into the operation control of the solar thermal subsystem and the photovoltaic subsystem. The control principle is to prioritize solar energy utilization. For the solar thermal subsystem, there are three heating modes: solar direct heating mode, solar-heat pump combined heating mode, and air-source heat pump heating mode. The control strategy is mainly based on differential temperature circulation to maximize solar energy utilization.

1) Solar direct heating mode: When the outlet temperature of the collector is 8 ℃ higher than the minimum tank temperature and the temperature of the heat storage tank is higher than 40 ℃, it indicates sufficient solar irradiance and

a relatively high supply temperature of the heat storage tank. After heat exchange, the working fluid can flow directly into the terminal heating equipment. In this case, only the solar heat collection loop is activated while the air-source heat pump is shut down, and heating is fully supplied by solar energy.

2) Solar-heat pump combined heating mode: When the outlet temperature of the collector is 8 ℃ higher than the minimum tank temperature but the temperature of the heat storage tank is lower than 40 ℃, there is a certain amount of solar irradiance yet insufficient. The air-source heat pump system is required for joint heating. At this time, both the solar heat collection loop and the air-source heat pump are turned on simultaneously to meet the heating demand.

3) Air-source heat pump heating mode: When the outlet temperature of the collector is 2 ℃ lower than the minimum tank temperature and the temperature of the heat storage tank is below 40 ℃, the solar irradiance is insufficient and unavailable. Under this condition, only the air-source heat pump is activated and the solar heat collection loop is shut down. The air-source heat pump is regulated to maintain the normal operation of the heating system. To guarantee the supply water temperature, the heating loop adjusts the primary supply water temperature by controlling the bypass flow rate. In this system, a three-way valve installed at the primary inlet of the plate heat exchanger is adopted for regulation to stabilize the outlet water temperature of the system.

3 ENGINEERING BACKGROUND

3.1 Meteorological Parameters of Yinchuan

This paper adopts meteorological parameters of a rural area in Yinchuan, Ningxia Hui Autonomous Region. Yinchuan is located at 106°20′ E, 38°30′ N. Monthly meteorological data of Yinchuan are exported via the Meteonorm meteorological data software, as shown in Figure 3 and Figure 4 below.

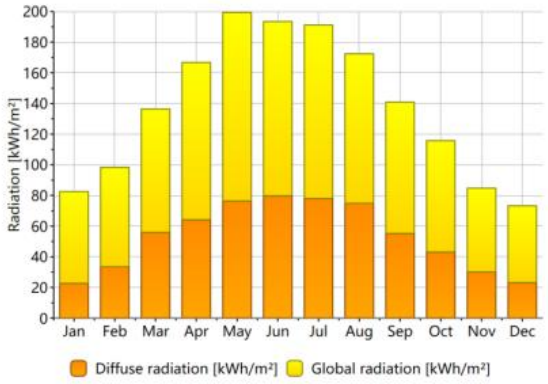


Figure 3 Solar Irradiance Distribution in Yinchuan

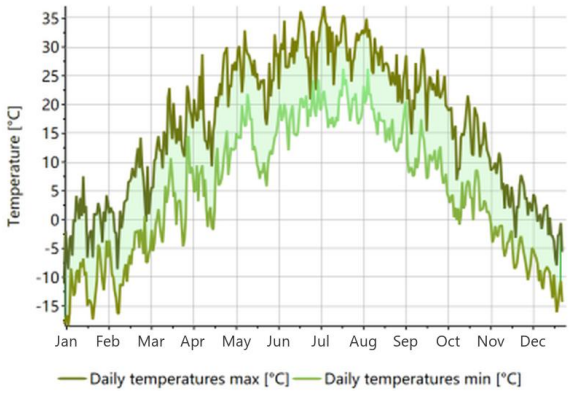


Figure 4 Annual Temperature Distribution in Yinchuan

3.2 Building Information

A typical single-story rural residence in Yinchuan, Ningxia, is selected as the research object. The net heating area of the building is 79.2 m² with a floor height of 3.3 m. Thermal insulation measures are not considered. The parameters of the building envelope are shown in Table 1 below.

Table 1 Building Envelope Parameters

Heat transfer coefficient of external wall (W/m²·K)	Heat transfer coefficient of roof (W/m²·K)	Thermal resistance of floor (m²·K/W)	Heat transfer coefficient of external window (W/m²·K)	Solar heat gain coefficient of external window	Heat transfer coefficient of external door (W/m²·K)

Heat transfer coefficient of external wall (W/m²·K)	Heat transfer coefficient of roof (W/m²·K)	Thermal resistance of floor (m²·K/W)	Heat transfer coefficient of external window (W/m²·K)	Solar heat gain coefficient of external window	Heat transfer coefficient of external door (W/m²·K)
0.524	0.475	2.146	2.015	0.60	0.703

4 SYSTEM SIMULATION AND RESULT ANALYSIS

The model consists of building module, solar collector module, meteorological data module, air-source heat pump unit module, water tank module, control system module and so on. Using the typical meteorological year data in TRNSYS, this paper simulates the room heat load and heating performance during the whole heating season from November 1st to March 31st of the next year (Figure 5).

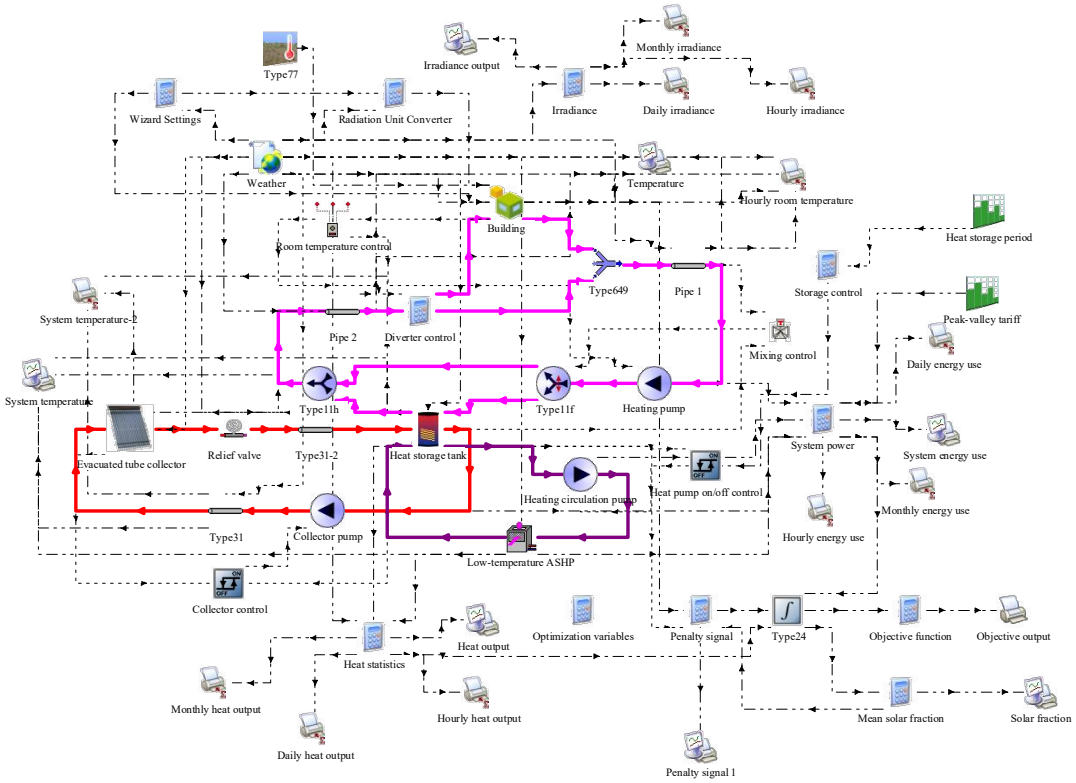


Figure 5 System Simulation Model Diagram

4.1 Temperature Characteristic Analysis

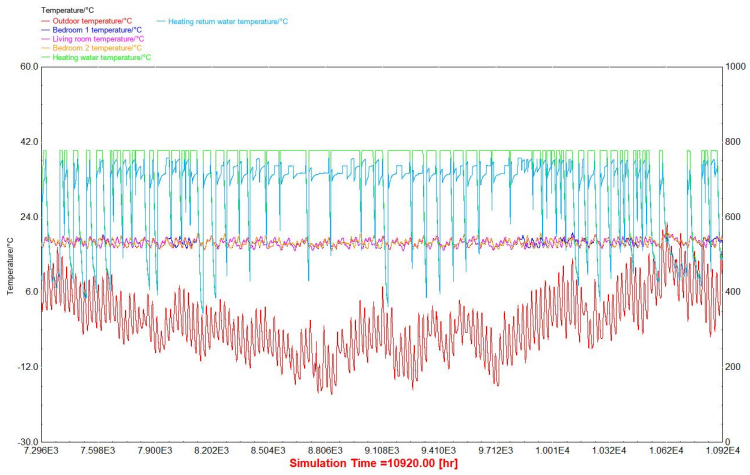


Figure 6 Indoor Temperature Distribution During the Heating Period

The temperature distribution of the coupled heating system during the heating period is shown in Figure 6. The horizontal axis represents time, ranging from 7296 h to 10920 h, corresponding to the heating period from November 1st to March 31st of the next year, which is the official heating period in Yinchuan, Ningxia. The red curve denotes outdoor temperature; dark blue and orange curves represent the temperatures of Bedroom 1 and Bedroom 2 respectively;

the pink curve indicates the living room temperature; the green curve stands for heating supply water temperature, and the light blue curve represents return water temperature.

It can be seen from Figure 6 that the outdoor temperature shows obvious seasonal fluctuations. The temperature is relatively low in December and January, with a minimum value of −18 °C, while it is higher in November and March, with a maximum value of 21 °C. The overall temperature fluctuates in a wide range, which imposes high requirements on the regulation of heating stability for the heating system. In general, the three indoor temperature curves overlap significantly. The indoor temperature is stably maintained within the comfortable range of 17–19 °C throughout the heating season, without sharp drops or overheating, indicating favorable temperature control performance of the system. Even when the outdoor temperature drops to the lowest level of −18 °C, the indoor temperature only fluctuates slightly and does not fall far below 17 °C. This demonstrates that the combined heating mode of solar energy coupled with air-source heat pump can adequately meet the building heating load under extreme cold conditions in Yinchuan.

4.2 Analysis of the System's Monthly Power Consumption Characteristics

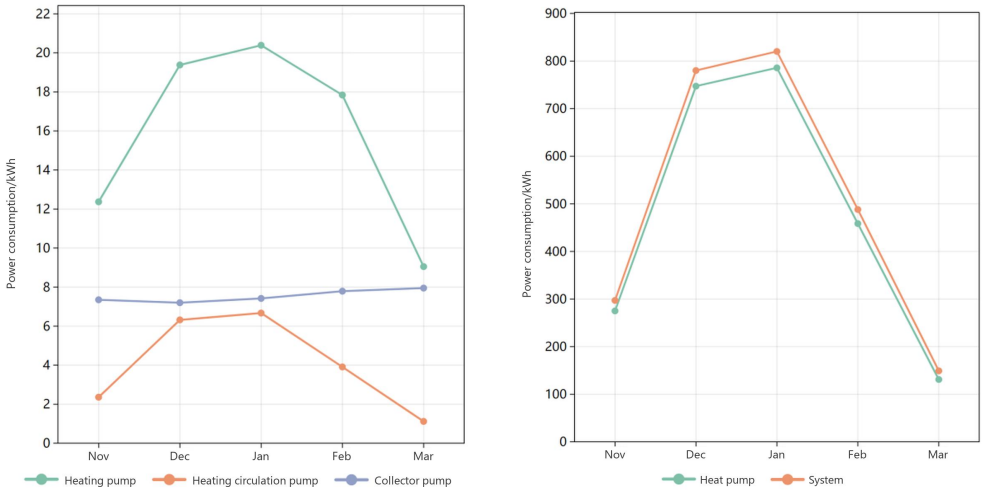


Figure 7 Monthly Electricity Consumption of the System and Its Major Power-Consuming Equipment

Combined with the curves in Figure 7, it can be observed that the outdoor temperature is relatively high in the early heating stage of November, resulting in low monthly power consumption of both the heating pump and the heating circulation pump. When entering the extreme cold period of December and January, the ambient temperature gradually decreases, and the building heat dissipation load reaches its annual peak. The power consumption of the two pumps rises progressively and peaks in January, with maximum monthly power consumption of 20.39 kWh and 6.67 kWh respectively. In February, the temperature rises and the heat load declines, so the power consumption decreases gradually. In March, the late heating period, the outdoor temperature increases and the heating operating duration is greatly shortened. The power consumption of the heating pump drops to 9.05 kWh, and that of the heating circulation pump falls to 1.12 kWh, which are the minimum values in the respective heating cycles. During the whole heating season, the total power consumption of the heating pump and heating circulation pump are 79.03 kWh and 20.38 kWh, accounting for 3.12% and 0.8% of the total system power consumption, respectively.

The variation trends of the two energy consumption indicators for the heat pump and the system are completely synchronized, showing an overall unimodal distribution characteristic of high in the middle and low at both ends, which is related to the winter temperature variation in Yinchuan, Ningxia. In November, the outdoor temperature is relatively high, the building heating heat load is small, and the power consumption is low. December and January witness the lowest temperatures of the whole year; the heat loss from building envelope heat dissipation and cold air infiltration increases significantly, and the heat pump operates under full-load heating conditions for a long time, so its energy consumption reaches the peak of the entire heating season. In February, the temperature rises slightly, the heating heat load decreases, and the total energy consumption of the heat pump and the system drops synchronously. In March, the outdoor temperature rises remarkably, the heating demand is greatly reduced, the operating duration of the heat pump decreases significantly, and the energy consumption falls to the minimum value of the whole cycle.

In summary, over the entire heating cycle, the total power consumption of the system is 2534.65 kWh, and the total power consumption of the heat pump is 2397.51 kWh. The heat pump accounts for 94.59% of the total system power consumption, while the auxiliary pumps only account for 5.41% of the total system energy consumption. The energy consumption of the whole system is dominated by the heating load of the air-source heat pump.

4.3 Monthly System Heat Analysis

Table 2 Monthly Solar Thermal Collection Efficiency and Solar Energy Availability Rate

Month	November	December	January	February	Mar	Average value
Solar thermal collection efficiency	44.08%	44.06%	46.33%	48.13%	42.00%	43.48%

Month	November	December	January	February	Mar	Average value
Solar energy guarantee rate	60.17%	39.42%	42.69%	53.72%	78.15%	49.67%

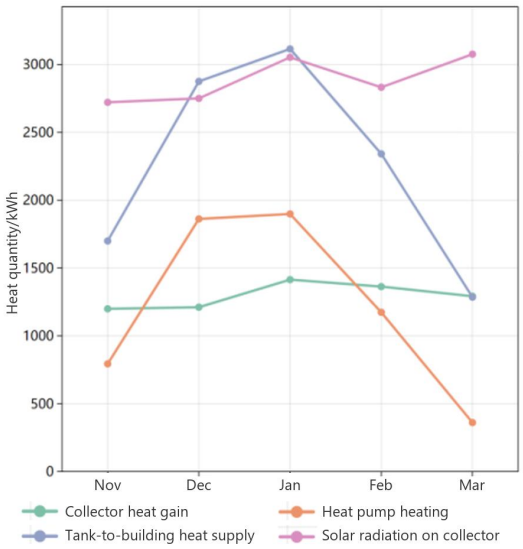


Figure 8 Monthly Heat Distribution of the System

Across the entire heating season, the heat collector generated 6,276.26 kWh of heat, while the air-source heat pump provided 6,359.19 kWh of heating; the two sources were nearly evenly distributed, and the total heat output of the heat pump was slightly higher than that of the solar collector. However, during the severe cold month of January, the heat pump's operating load was excessively high, resulting in a relatively heavy dependence on electricity. To further reduce carbon emissions and save electricity, in addition to the off-peak electricity-based thermal storage designed for this system, the heat-collection area could be expanded to increase solar heat generation during the severe cold periods of December and January, thereby reducing the peak heating load of the heat pump (Table 2; Figure 8).

4.4 Monthly Energy Efficiency Analysis of the Heat Pump and System

Table 3 Heat Pump COP and System Energy Efficiency Ratio

Month	November	December	January	February	Mar	Average value
Heat pump COP	2.89	2.49	2.42	2.56	2.76	2.33
System Energy Efficiency Ratio	5.72	3.69	3.80	4.80	8.62	3.95

During the heating season, the heat pump COP follows a pattern of being high at the beginning and end of the heating period and relatively low in deep winter: the COP reaches its peak of 2.89 in November, its lowest value of 2.42 in January, and an average of 2.33 over the heating season. The system's energy efficiency ratio is influenced by the solar energy availability rate; its trend differs from that of the heat pump COP. Solar energy supply accounts for the highest proportion in March, when the system's energy efficiency ratio reaches 8.62; in December, it falls to 3.69, while the system's average energy efficiency ratio is 3.95 (Table 3).

4.5 Analysis of the System's Environmental Performance

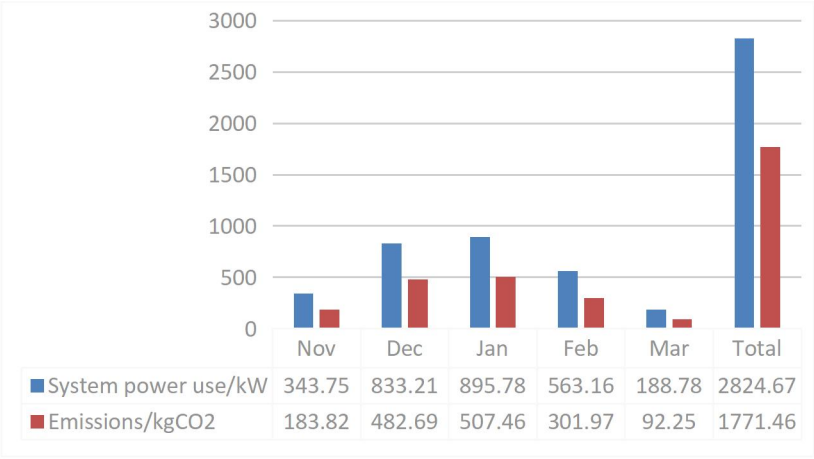


Figure 9 Systemic Monthly Carbon Emissions

The monthly trend in system carbon emissions exhibits pronounced seasonal variation, driven by outdoor temperature and building heat load. In January, outdoor temperatures are at their lowest, and building heating demand reaches its peak; system carbon emissions amount to 507.46 kg CO_2, the highest value during the heating cycle. In March, temperatures rise and heat-load demand drops sharply, reducing carbon emissions to 92.25 kg CO_2, the lowest value during the heating cycle; in November and February, temperatures remain moderate, resulting in intermediate carbon emissions. Cumulative system carbon emissions during the heating season total 1,771.46 kg CO_2; because solar thermal collection offsets part of the electricity demand, total carbon emissions are significantly reduced (Figure 9).

4.6 Comparison of Carbon Emissions Between Coupled Heating Systems and Conventional Heating Systems

Table 4 Comparison of Carbon Emissions Between Coupled Systems and Conventional Heating Systems

Heating method	System energy conversion efficiency	Energy consumption	Carbon emission kgCO_2
Solar-powered CO_2 heat pump heating	3.95	electric energy: 2317.67 kWh	1433.94
Independent heat pump heating	2.2	electric energy: 4161.27 kWh	2574.58
Coal-fired boiler heating	0.7	coal: 2249.49 kg	5848.67
Electric heating	1	electric energy: 9154.79 kWh	5664.07

As shown in Table 4, the four heating methods are ranked from lowest to highest carbon emissions as follows: solar-assisted CO_2 heat pump heating, standalone heat pump heating, electric heating, and coal-fired boiler heating. Solar-assisted heat pump heating emits only 1,433.94 kg of CO_2, which is 24.5% of the emissions from coal-fired boilers (the highest level), 25.3% of those from electric heating, and 55.7% of those from standalone heat pumps; thus, its effectiveness in reducing carbon emissions and energy consumption is significant.

5 CONCLUSION

This study takes a typical single-story rural residence in Yinchuan, Ningxia, as its research subject. Using TRNSYS software, a simulation model for a solar–CO_2 air-source heat pump combined with valley electricity-based thermal storage heating system was developed. The system's operating characteristics throughout the entire heating season, from November 1 to March 31 of the following year, were simulated and analyzed. The main conclusions are as follows:

(1) Throughout the entire heating season, the indoor temperature of the coupled system remained stably within the comfortable range of 17-19℃; even when the outdoor temperature dropped to -18℃, the amplitude of indoor temperature fluctuations was kept within 2℃, with no instances of severe underheating or overheating occurring; the supply water temperature remained essentially stable at approximately 40℃; temperature consistency across rooms with different functions was excellent; and the system's temperature control performance was satisfactory, enabling it to fully meet the building heating load under the extremely cold conditions of the Yinchuan region.

(2) The system's total electricity consumption over the entire heating cycle was 2,534.65 kWh, of which the air-source heat pump consumed 2,397.51 kWh, accounting for 94.59% of total electricity consumption; the auxiliary pump consumed only 5.41% of the total electricity, and the system's energy consumption was dominated by the heating load of the air-source heat pump.

(3) During the heating season, the total heat collected by the collectors was 6,276.26 kWh, while the total heating output of the air-source heat pump was 6,359.19 kWh; the two values are nearly equal, and the total heat produced by the heat pump is slightly higher than that produced by solar collection, reflecting the design strategy of "prioritizing solar energy and using heat pumps for peak-shaving and supplementary heating." The system's average solar collection efficiency was approximately 43.48%, and the average solar availability rate was 49.67%. During the severe cold month of January, the heat pump operating load was excessively high and its dependence on electricity was relatively large; therefore, expanding the collection area could be considered to increase solar heat generation during the severe cold period and reduce the peak heating load of the heat pump.

(4) During the heating season, the heat pump COP follows a pattern of being high at the beginning and end of the heating period and relatively low in deep winter: it reaches a maximum of 2.89 in November, a minimum of 2.42 in January, and an average of 2.33 during the heating season; the system's energy efficiency ratio is influenced by the solar energy guarantee rate, reaching a maximum of 8.62 in March and a minimum of 3.69 in December; the system's average energy efficiency ratio is 3.95, indicating that the overall system energy efficiency is good.

(5) During the system heating season, cumulative carbon emissions amounted to 1,771.46 kg CO_2, with a peak of 507.46 kg CO_2 in January and a minimum of 92.25 kg CO_2 in March; carbon emissions during the two deep-winter months of December and January accounted for 55.9% of total emissions during the heating season, making this period the core phase for system emission reduction and optimization. By increasing the solar thermal storage capacity and extending the duration of thermal storage during off-peak electricity hours, daytime peak electricity consumption can be reduced. Compared with conventional heating methods, solar-coupled heat-pump heating resulted in carbon emissions

of only 1,433.94 kg CO_2, 24.5% of those from coal-fired boiler heating, 25.3% of those from electric heating, and 55.7% of those from standalone heat-pump heating—demonstrating significant carbon reduction and energy consumption savings.

COMPETING INTERESTS

The authors have no relevant financial or non-financial interests to disclose.

FUNDING

This work was supported by the Key Scientific Research Project of Yinchuan University of Energy (Grant No. 2023-KY-Z-6), titled Research on Heating Performance of Solar-CO_2 Air Source Heat Pump System.

REFERENCES

[1] Ye J J, Hu H T, Ding G L, et al. Performance analysis of solar-assisted CO_2 ground-source heat pump system. Refrigeration Technology, 2016, 36(1): 1-6.
[2] Zheng Y X, Zhao S, Li J. Characteristic analysis and evaluation of solar-air source heat pump composite heating system applied in Xi'an. Solar Energy, 2021, (2): 36-43.
[3] Wang Y N, Wang F H. Performance comparison between parallel and series solar heat pump hot water systems. In: Proceedings of Chinese Association of Refrigeration Annual Conference, 2011: 347-351.
[4] Zeng N H, Yuan Y P, Sun L L, et al. Optimization study of air-source heat pump assisted solar hot water system based on TRNSYS. Acta Energiae Solaris Sinica, 2018, 39(5): 1245-1254.
[5] Zhang X R, Yamaguchi H. An experimental study on evacuated tube solar collector using supercritical CO_2. Applied Thermal Engineering, 2008, 28(10): 1225-1233.
[6] Kim W, Oh J, Park C, et al. Study on solar hybrid heat pump system using carbon dioxide. In: 23rd International Conference of Refrigeration, Prague, Czech Republic, 2011.
[7] Yang J L,Wu Y T, Wang C X, et al. Experimental study on transcritical CO_2 water to water heat pump system. Cryogenics & superconductivity, 2020, 48(4): 79- 84.
[8] Yang L X. Experimental study on characteristics of transcritical CO_2 heat pump system and influencing factors of outlet water temperature. Zhengzhou: Zhengzhou University, 2019.